13.9%-Efficiency and Eco-Friendly Nonfullerene Polymer Solar Cells Obtained by Balancing Molecular Weight and Solubility in Chlorinated Thiophene-Based Polymer Backbones

*Sung Jae Jeon, Yong Woon Han, and Doo Kyung Moon**

To industrialize nonfullerene polymer solar cells (NFPSCs), the molecular design of the donor polymers must feature low-cost materials and a high overall yield. Two chlorinated thiophene-based polymers, P(F–Cl) and P(Cl–Cl), are synthesized by introducing halogen effects like fluorine (F) and chlorine (Cl) to the previously reported P(Cl), which exhibits low complexity. However, the molecular weights of these polymers are insufficient owing to their low solubility, which in turn is caused by introducing rigid halogen atoms during the polymerization. Thus, they show relatively low power conversion efficiencies (PCEs) of 11.8% and 10.3%, respectively. To overcome these shortcomings, two new terpolymers are designed and synthesized by introducing a small amount of 1,3-bis(5-bromothiophen-2-yl)-5,7-bis(2-ethylhexyl)benzo[1,2-c:4,5-c']dithiophene-4,8-dione (BDD) unit into each backbone, namely, P(F–Cl)(BDD = 0.2) and P(Cl–Cl)(BDD = 0.2). As a result, both polymers remain inexpensive and show a better molecular weight–solubility balance, achieving high PCEs of 12.7% and 13.9%, respectively, in NFPSCs processed using eco-friendly solvents.

1. Introduction

Recently, polymer solar cells (PSCs) have achieved power conversion efficiencies (PCEs) greater than 16%[1–4] and 17%[5] in single and tandem solar cells, respectively, owing to the innovative development of nonfullerene acceptors (NFAs).[6–11] Despite this impressive achievement, the high costs of raw materials and device fabrication remain unresolved impediments to the industrialization of PSCs.[12,13] In particular, π-conjugated donor polymers are required to reduce the synthetic complexity (SC), including the number of steps, overall yields, and costs of raw materials and final products.[14,15] Accordingly, we previously proposed a strategy for designing wide-bandgap donor polymers based on 2D benzo[1,2-b:4,5-b'] dithiophene (2DBDT)

and halogenated heterocycle rings,[16,17] which is a simple donor–acceptor (D–A) approach with a relatively low SC.[17] By introducing a 3-chlorothiophene (Cl–Th) unit, which has the deepest-lying highest occupied molecular orbital (HOMO) levels and strongest dipole moment among halogenated thiophenes, into the 2DBDT-based polymer backbone, we were able to develop a wide-bandgap donor polymer, P(Cl), with a PCE of up to 12.1% and a relatively lower cost than that of existing D–A donor polymers.[17] To achieve PSCs that outperform those with P(Cl), we consider introducing donor units substituted with F or Cl instead of nonhalogenated 2DBDT into the polymer backbone.[18–21] However, because relatively bulky, rigid halogen atoms were introduced when using the restricted alkyl side chains to dissolve their polymer backbones, the molecular weight and solubility decreased during polymer chain growth. This can ultimately degrade the photovoltaic performance.[22–25] In these cases, the insufficient lengths of alkyl side chains should be increased or π–spacers introduced to provide appropriate molecular weights to realize the desired structure–property relationship.[22,26–28] However, such techniques not only increase the synthetic complexity but may overmuch change the crystallinity and orientation properties of the polymers at times, which therefore must be carefully considered.[22,29] Therefore, developing a reasonable technique to balance molecular weight with solubility is paramount to driving the inherent properties of D–A donor polymers for high-efficiency PSCs.

Herein, we present new designs for four 2DBDT-chlorinated thiophene-based donor polymers. First, we design and synthesize two donor polymers based on fluorinated/chlorinated 2DBDT (F–2DBDT/Cl–2DBDT), denoted by P(F–Cl) and P(Cl–Cl), respectively, for simplicity, by modifying the structure of P(Cl). However, P(F–Cl) and P(Cl–Cl) polymers have lower molecular weight than P(Cl), and the structure–property potential of the polymers based on the introduction of F and Cl is not expressed. Thus, combining these polymers with 3,9-bis(2-methylene-((3-(1,1-dicyanomethylene)-6,7-difluoro)-indanone))-5,5,11,11-tetrakis(4-hexylphenyl)-dithieno[2,3-d:2',3'-d']-s-indaceno[1,2-b:5,6-b']dithiophene (IT-4F) in the

Dr. S. J. Jeon, Dr. Y. W. Han, Prof. D. K. Moon
Nano and Information Materials (NIMs) Laboratory
Department of Chemical Engineering
Konkuk University
120, Neungdong-ro, Gwangjin-gu, Seoul 05029, Korea
E-mail: dkmoon@konkuk.ac.kr
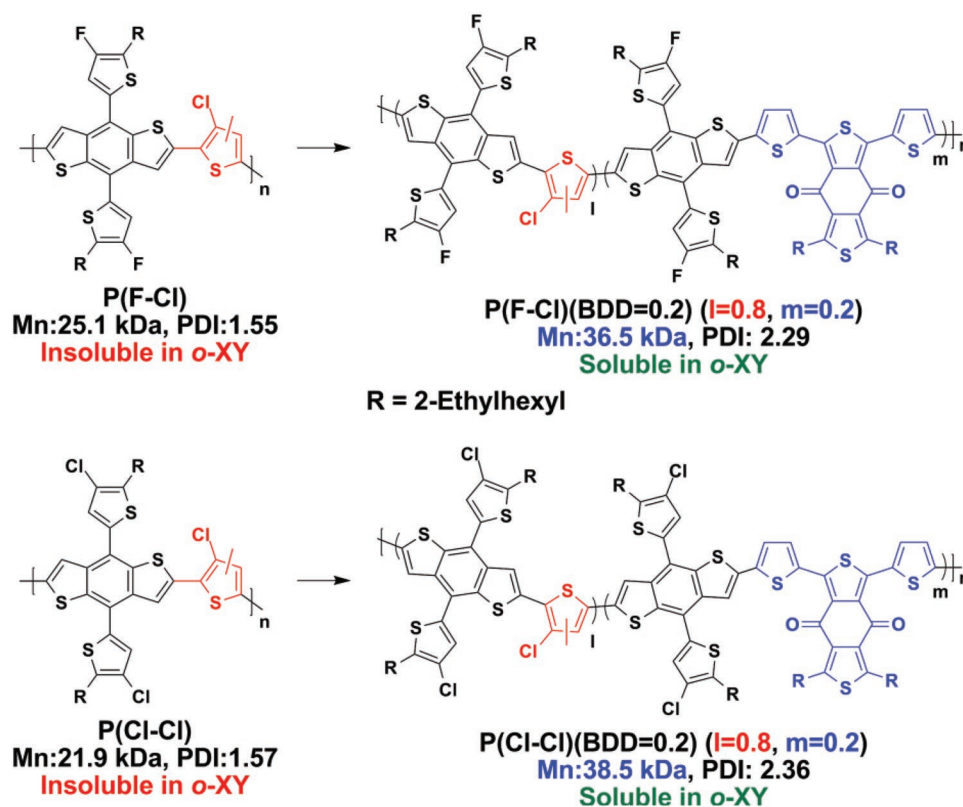
Scheme 1. Summary for synthetic donor polymers.

PSCs results in PCEs of 11.8% and 10.3%, respectively. To challenge this problem, we attempt to synthesize different terpolymers by introducing a small amount of 1,3-bis(5-bromothiophen-2-yl)-5,7-bis(2-ethylhexyl)benzo[1,2-c:4,5-c′]dithiophene-4,8-dione (BDD) instead of Cl–Th as the acceptor unit in the polymer backbones: P(F–Cl)(BDD = 0.2)–F–2DBDT:Cl–Th:BDD = 1:0.8:0.2 and P(Cl–Cl)(BDD = 0.2)–Cl–2DBDT:Cl–Th:BDD = 1:0.8:0.2. The BDD unit has a higher SC than Cl–Th, but only a trace amount of 20 mol% is introduced; thus, this attempt is believed to be more advantageous from a figure-of-merit (FOM = SC/PCE) standpoint, i.e., when the increase in efficiency is greater than the increase in cost.[14,30–32] Moreover, it is predicted that the BDD unit does not cause steric hindrance when introduced into F–2DBDT/Cl–2DBDT-chlorinated thiophene-based polymer backbones, and it also decreases the bandgap of the polymer and maintains similar HOMO levels.[20,21,33]

Consequently, P(F–Cl)(BDD = 0.2) and P(Cl–Cl)(BDD = 0.2) terpolymers show higher molecular weights and solubility than P(F–Cl) and P(Cl–Cl). IT-4F-based PSCs show high-efficiency PCEs of 12.7% and 13.2%, respectively, owing to the improved physical, optical, and orientation of these terpolymers. Moreover, even when fabricated with nonchlorinated solvents (o-xylene (XY)/1-phenylnapthalene (PN)), the PSCs show superior PCEs of 12.2% and 13.5%, respectively, owing to the balance between molecular weight and solubility of P(F–Cl)(BDD = 0.2) and P(Cl–Cl)(BDD = 0.2). Notably, both devices were certified by the Nano Convergence Practical Application Center (NCPAC) in Korea, and they achieved the highest PCEs

of 12.70% and 13.97%, thus confirming our development of high-performance, eco-friendly NFPSCs.

2. Results and Discussion

2.1. Design, Theoretical Calculations, and Physical Properties

We focused on the development of high-efficiency donor polymers with balanced molecular weight and solubility by modifying and optimizing the structure of P(Cl).[17] P(Cl) was characterized and reported in our previous work.[17] As shown in **Scheme 1**, we designed and synthesized four chlorinated thiophene-based donor polymers, namely, P(F–Cl), P(F–Cl)(BDD = 0.2), P(Cl–Cl), and P(Cl–Cl)(BDD = 0.2). In particular, the two polymers with BDD units showed a relatively high yield in the chloroform fraction (they perfectly dissolved in chloroform.) during Soxhlet extraction. The synthesis method and characterizations of the polymers are described in detail in the Supporting Information (Scheme S1 and Figures S1–S4, Supporting Information). All donor polymers dissolved well in common chlorinated organic solvents such as chloroform, chlorobenzene, and o-dichlorobenzene. However, P(F–Cl) and P(Cl–Cl) almost did not dissolve in nonchlorinated solvents such as toluene and o-xylene, whereas P(F–Cl)(BDD = 0.2) and P(Cl–Cl)(BDD = 0.2) showed good solubility, completely dissolving at 25 °C.

Firstly, density functional theory (DFT) calculations for donor polymers were performed with the model structures, as shown

ADVANCED
SCIENCE NEWS

www.advancedsciencenews.com

NANO · MICRO
small
www.small-journal.com

in Scheme S2 in the Supporting Information, (Figures S5 and S6 and Table S1, Supporting Information). In the case of P(F–Cl)(BDD = 0.2) and P(Cl–Cl)(BDD = 0.2), simulating structures most similar to actual polymers would require performing the calculations on the model compounds of (repeating unit, $n = 1$: P(F–Cl)(BDD = 0.2) and P(Cl–Cl)(BDD = 0.2)) combined with ($n = 2$: P(F–Cl) and P(Cl–Cl)), respectively. Therefore, because of the exponential increase in time, calculations for P(F–Cl)(BDD = 0.2) and P(Cl–Cl)(BDD = 0.2) were performed and analyzed by substituting the model compounds of ($n = 1$: P(F–Cl)(BDD = 0.5) and P(Cl–Cl)(BDD = 0.5) by introducing 50 mol% BDD as acceptor units), respectively. As shown in Figure S5 and Table S1 (Supporting Information), Cl–2DBDT-based P(Cl–Cl) showed a slightly lower HOMO level and wider bandgap than F–2DBDT-based P(F–Cl) owing to higher electron density.[21] As the BDD unit was introduced into each F–2DBDT/Cl–2DBDT-chlorinated thiophene-based polymer backbone, the bandgap P(F–Cl)(BDD = 0.2) and P(Cl–Cl)(BDD = 0.2) tended to decrease because both the HOMO and lowest unoccupied molecular orbital (LUMO) levels shifted lower. As shown in Table S1 (Supporting Information), the curvatures of model compounds showed θ_1, θ_2, and θ_3 values tilting in the positive direction, and as BDD units were introduced, the sum of these three values decreased. Based on this finding, the polymers were predicted to show increasing planarity in the order of P(Cl–Cl) < P(F–Cl) < P(Cl–Cl)(BDD = 0.2) < P(F–Cl)(BDD = 0.2). Moreover, as BDD units were introduced into the polymer backbones, intermolecular π–π stacking was expected to improve owing to the increasing length of curvature (L) of the polymers.[34,35] Lastly, when the electrostatic potentials (ESPs) of donor polymers were calculated, the results showed predominantly positive continuous potentials along the π-conjugated polymer main backbones in all polymers, which would be expected to provide efficient charge transport (Figure S6, Supporting Information).[17] The calculated values are summarized in detail in Table S1 (Supporting Information).

The gel permeation chromatography (GPC) results of the donor polymers showed that P(F–Cl) and P(Cl–Cl) had number-average molecular weights (M_n) below ≈25.1 kDa, with relatively low solubility due to the introduction of F and Cl, respectively, and the restricted alkyl side chains. On the other hand, both P(F–Cl)(BDD = 0.2) and P(Cl–Cl)(BDD = 0.2) showed increased molecular weights of ≥36.5 kDa based on their excellent solubility. In the thermogravimetric analysis (TGA), the temperature at which a 5% weight loss occurred (T_d) was relatively higher in both polymers with BDD units owing to their higher aromaticity (Figure S7, Supporting Information).

Lastly, differential scanning calorimetry (DSC) was performed to analyze the crystallinity of the donor polymers at 30–270 °C, and the results showed no peaks indicating differences in crystallinity (Figure S8, Supporting Information).[33] The results of these analyses are summarized in **Table 1**.

2.2. Optical and Electrochemical Properties

As shown in **Figure 1**, the optical and electrochemical properties of donor polymers were investigated through UV–visible spectroscopy (UV–vis) and cyclic voltammetry (CV). To understand the optical and electrochemical interactions between donor polymers, IT-4F was also analyzed in this study. As shown in Figure 1a,b, donor polymers in both the solution and film states showed two absorption peaks at 300–400 and 400–650 nm based on π–π^* transition intramolecular charge transfer (ICT) between the donor and chlorinated thiophene units of the donor polymers, whereas IT-4F showed a single absorption band at 600–800 nm, indicating strong ICT effects.[16–19,36] Therefore, complementary light absorption in blends could be expected from the four donor polymers and IT-4F.[18,19,21]

As shown in Figure S9 and S10 (Supporting Information), UV–vis measurements were taken in four dilute chloroform solution states at different concentrations on the order of 10^{-5} M. When these were substituted into the Beer–Lambert equation,[16,17,37] the average molar absorption coefficients (ε) of the polymers with BDD tended to increase more than those of the polymers without BDD. This difference is attributable to the extended π-conjugation length and increased molecular weight relative to those of the Cl–Th unit.[16,20,21] As the F–2DBDT-based donor polymers changed from a solution state to a film state, their peak intensities red-shifted as the intermolecular distance decreased.[18,21] On the other hand, Cl–2DBDT-based donor polymers showed a decrease in shoulder peaks indicating π–π stacking effects in the film state owing to the introduction of relatively bulky Cl–2DBDT into the polymer backbones.[19,21] However, this tendency was lessened in P(F–Cl)(BDD = 0.2) and P(Cl–Cl)(BDD = 0.2) owing to decreased intramolecular steric hindrance and increased L owing to the BDD in the polymer backbone. These results agree well with previous computational simulation results. Both polymers showed relative decreases in the optical bandgaps (E_g^{opt}), also agreeing with the computational simulations. This finding means that devices fabricated with these polymers could attain a higher short-circuit current density (J_{sc}) than devices with P(F–Cl) and P(Cl–Cl).[21] Lastly, in the CV measurements, the donor polymers showed HOMO levels decreasing in the order of P(F–Cl)(BDD = 0.2) > P(F–Cl) > P(Cl–Cl)(BDD = 0.2) > P(Cl–Cl), with values of −5.62, −5.64, −5.67, and −5.70 eV, respectively (Figure S11, Supporting Information). When all donor polymers were blended with the deeper-lying HOMO levels of IT-4F −5.71 eV, we expected to see good energy level alignment, as shown in Figure 1c.[18–21] The optical and electrochemical properties of
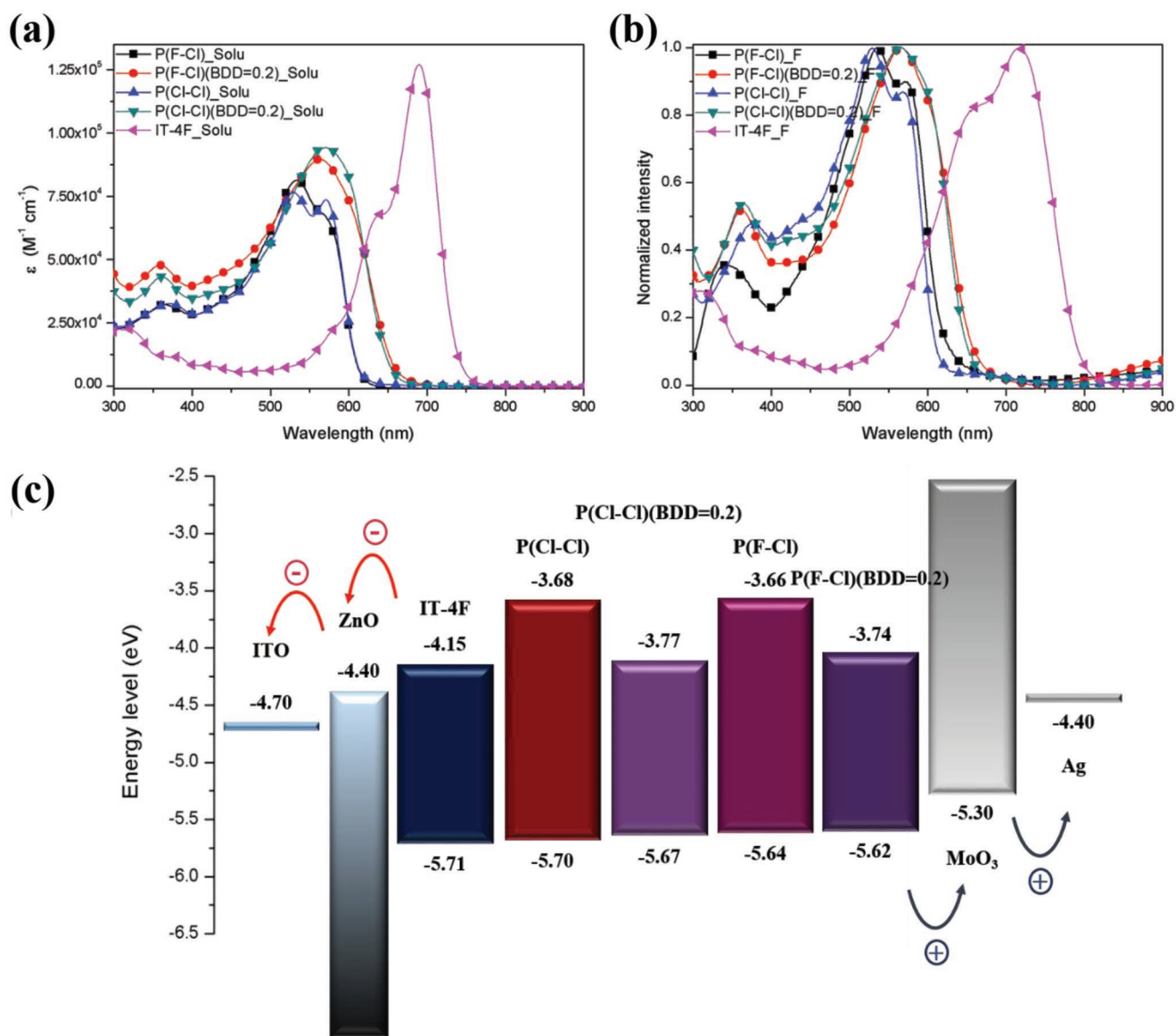
Table 1. Physical and thermal properties of donor polymers.

Polymer	Yield [%]	M_n[a] [kDa]	M_w[a] [kDa]	PDI[a]	T_d[b] [°C]
P(F–Cl)	77.0	25.1	38.8	1.55	365
P(F–Cl)(BDD = 0.2)	85.0	36.5	83.6	2.29	386
P(Cl–Cl)	72.0	21.9	34.3	1.57	364
P(Cl–Cl)(BDD = 0.2)	89.0	38.5	91.0	2.36	372

[a]Parameters (M_n: number-average molecular weight; M_w: weight-average molecular weights; PDI: polydispersity index) determined via GPC in chloroform using polystyrene standards; [b]Temperature resulting in 5% weight loss based on the initial weight.

Figure 1. UV–vis absorption spectra and energy band diagrams from CV curves of donor polymers and IT-4F: a) average molar absorption coefficients for 10^{-5} diluted chloroform solutions, b) UV–vis absorption spectra of chloroform solutions versus thin films, and c) energy band diagrams of donor polymers and IT-4F in the inverted devices.

the donor polymers are summarized in **Table 2**, and those of IT-4F are summarized in Table S2 (Supporting Information).

2.3. Photovoltaic Performance

Devices were fabricated in the inverted configurations of ITO/ZnO/polymer:IT-4F/MoO$_3$/Ag, and to obtain more stable devices than conventional devices, a metal anode with a higher work function was used.[38] First, the devices with P(F–Cl):IT-4F, P(F–Cl)(BDD = 0.2), P(Cl–Cl):IT-4F, and P(Cl–Cl)(BDD = 0.2) were optimized with chlorinated solvents: chlorobenzene (CB):1,8-diiodooctane (DIO) = 99.5:0.5, v/v %. (The detailed process is shown in the Supporting Information.) The current density–voltage (J–V) and external quantum

efficiency (EQE) curves of the optimized polymer blends for PSCs are displayed in **Figure 2**a,b, respectively, and the associated parameters are listed in **Table 3**. As a result, P(F–Cl):IT-4F and P(Cl–Cl):IT-4F showed the highest PCEs of 11.8% and 10.2%, respectively. Although these polymers were expected to perform better than P(Cl) owing to the effects of F and Cl, high performance was not achieved owing to a low fill factor (FF), in contrast with the relatively high open-circuit voltage (V_{oc}) and J_{sc}. On the other hand, P(F–Cl)(BDD = 0.2):IT-4F and P(Cl–Cl)(BDD = 0.2):IT-4F, which had higher molecular weights, achieved higher PCEs of 12.7% and 13.2%, respectively, owing to increases in both J_{sc} and FF. In particular, both polymers showed EQEs over 85% at 550–750 nm, the high ratio of the number of photogenerated charges collected to the number of incident photons in maximum absorption spectra

ADVANCED
SCIENCE NEWS
www.advancedsciencenews.com

NANO · MICRO
small
www.small-journal.com

Table 2. Optical and electrochemical properties of donor polymers.

Polymer	UV–visible absorption			Cyclic voltammetry			
	Chloroform solution	Molar absorption coefficient	Film	$E_g^{opt,a}$ [eV]	E_{ox}^{onset} [V]	$E_{HOMO}^{b,c}$ [eV]	E_{LUMO}^{b} [eV]
	λ_{max} [nm]	ε [M^{-1} cm^{-1}] at λ_{max} [nm]	λ_{max} [nm]				
P(F–Cl)	361, 533	32172 (361), 81299 (533)	342, 535, 571	1.99	1.34	−5.64	−3.66
P(F–Cl)(BDD = 0.2)	359, 562	47730 (359), 89598 (562)	361, 565	1.88	1.32	−5.62	−3.74
P(Cl–Cl)	371, 529, 571	32580 (371), 76681 (529), 73711 (571)	375, 529, 568	2.02	1.40	−5.70	−3.68
P(Cl–Cl)(BDD = 0.2)	362, 571	43070 (362), 94402 (571)	364, 565	1.90	1.37	−5.67	−3.77

[a]Calculated from the intersection of the tangent of the low-energy edge of the absorption spectrum with the baseline; [b]$E_{HOMO} = -[E_{ox}^{onset}$ (vs Ag/AgCl) $- E_{1/2,ferrocene}$ (Fc/Fc$^+$ vs Ag/AgCl)^{c}] − 4.8 eV, $E_{LUMO} = E_g^{opt} - E_{HOMO}$; [c]$E_{1/2,ferrocene}$ (Fc/Fc$^+$ vs Ag/AgCl) = 0.49 eV (measured data).

of the donor and acceptor.[39,40] Notably, these results indicate that efficient charge collection and superior light-harvesting capability are possible, even in thin films with thicknesses of 100–110 nm.[39,40] This is in agreement with the results for P(F–Cl)(BDD = 0.2) and P(Cl–Cl)(BDD = 0.2) obtained in our laboratory with about 6.1% and 6.5% mismatches, respectively. As shown in Figure S12 (Supporting Information), the maximized optical density of each polymer blend is very close the maximized EQE values at 600 and 700 nm, respectively, suggesting that the light absorption of the donor and acceptor make good contribution to the current density of the devices. Plus, the internal quantum efficiency (IQE) of the P(F–Cl)(BDD = 0.2) and P(Cl–Cl)(BDD = 0.2)-based inverted devices has been measured based on reflectance (R) and EQE; the IQE spectra show very high values of nearly 90% in a range from 550 to 750 nm. The high IQE curve suggests that most absorbed photons create charge carriers that are collected at the electrodes.

2.4. Crystallinity and Orientation Analysis

2D grazing-incidence wide-angle X-ray scattering (2D GIWAXS) is an efficient approach for investigating the crystallinity and molecular orientation of pristine photoactive materials and optimized polymer blends.[17,41] As demonstrated in Figures S13 and S15 (Supporting Information) and **Figure 3**, the

2D GIWAXS patterns were used to obtain the corresponding out-of-plane (OOP; along q_z) (Figures S14a, S16a, and S17a, Supporting Information) and in-plane (IP; along q_{xy}) profiles (Figures S14b, S16b, and S17b, Supporting Information) of all films. In addition, we constructed intensity-integrated azimuthal pole figure plots for the (100) scattering peaks of the pristine and blended polymer films (Figures S14c, S16c, and S17c, Supporting Information). The integrated areas within the azimuthal angle (χ) in the ranges of 0°–45° (A_z) and 45°–90° (A_{xy}) are defined as the corresponding fractions of face-on and edge-on structures, respectively, and the ratio A_{xy}/A_z was calculated as a metric for the face-on-to-edge-on ratio. First, as demonstrated by A_{xy}/A_z, all pristine donor polymers except P(F–Cl)(BDD = 0.2) showed dominant face-on structures and similar orientations on the ZnO substrate. The d-spacing of (100) planes, which represents the lamellar packing of P(F–Cl)(BDD = 0.2) and P(Cl–Cl)(BDD = 0.2), increased when introducing only a small amount of BDD units, compared with those of P(F–Cl) and P(Cl–Cl). In the case of the (010) plane, representing π–π stacking distance, the d-spacing ($d[010]$) in P(F–Cl)(BDD = 0.2) was greater than that of P(F–Cl), whereas $d[010]$ in P(Cl–Cl)(BDD = 0.2) was smaller than that of P(Cl–Cl). As shown in the DFT calculations in Table S1 (Supporting Information), such differences may be attributable to the fact that both F–2DBDT units adjacent to Cl–Th showed increases in the tilting angles to 1.48° and 1.85°, respectively, in the segments
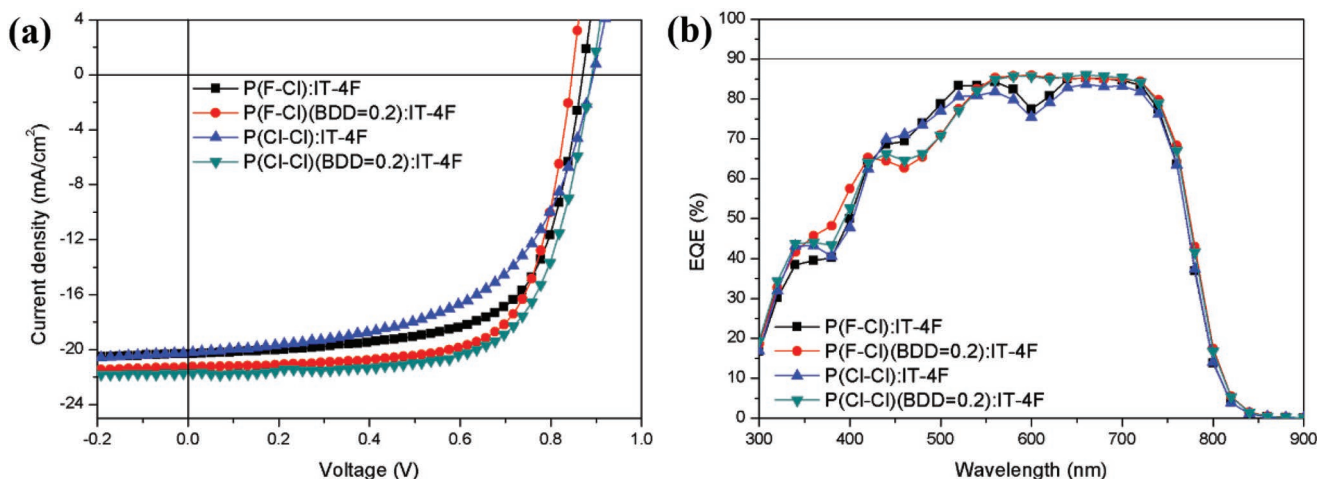

Figure 2. a) *J*–*V* and b) EQE curves of the optimized polymer blends for inverted PSCs.

Table 3. Optimized photovoltaic performance of inverted PSCs with polymer blends.

Active Layer	Thickness [nm]	Temperature[a] [°C]	V_{oc} [V]	J_{sc} [mA cm^{-2}]	FF [%]	PCE$_{max}$/PCE$_{ave}$[b] [%]
P(F–Cl):IT-4F = 1:1	95	140	0.879	20.3	66.0	11.8/11.5 ± 0.30
P(F–Cl)(BDD = 0.2):IT-4F = 1:1	100	150	0.838	21.3	71.0	12.7/12.5 ± 0.22
P(Cl–Cl):IT-4F = 1:1	110	160	0.899	20.3	56.1	10.2/10.0 ± 0.19
P(Cl–Cl)(BDD = 0.2):IT-4F = 1:1	110	160	0.899	21.7	67.5	13.2/12.9 ± 0.31

[a]Post-annealing for 10 min; [b]Average PCE values are calculated from ten individual cells.

of P(F–Cl)(BDD = 0.2) with the introduction of BDD units. In contrast, a decrease in tilting angles to 1.70° and 1.03° was observed in the segments of P(Cl–Cl)(BDD = 0.2). As an NFA, IT-4F showed a balanced structure between face-on and edge-on structures. When donor polymers and IT-4F were blended, all blends except those with P(Cl–Cl) and P(Cl–Cl)(BDD = 0.2) showed relatively greater d[100], while the d-spacing of (010), i.e., d[010], decreased in the order of P(F–Cl) > P(F–Cl)(BDD = 0.2) > P(Cl–Cl) > P(Cl–Cl)(BDD = 0.2). In addition, all blends except P(Cl–Cl):IT-4F increasingly tended to form the face-on structure over the edge-on structure. Especially in the case of

P(Cl–Cl)(BDD = 0.2), blending with IT-4F resulted in more densely packed (100) and (010) planes than its pristine state, as well as a significant increase in the face-on structure, as calculated by A_{xy}/A_z. These results support the photovoltaic performance of each polymer blend. Moreover, the crystal coherence length (CCL) at (100) and (010) were calculated, i.e., CCL(100) and CCL(010), and the results indicated that all blends tended to show higher CCL(100) and CCL(010) than pristine films. On the other hand, P(Cl–Cl)(BDD = 0.2):IT-4F showed a decrease in crystal size at (010), which indicated that crystals were relatively larger at (100) and that this sample had the highest crystallinity
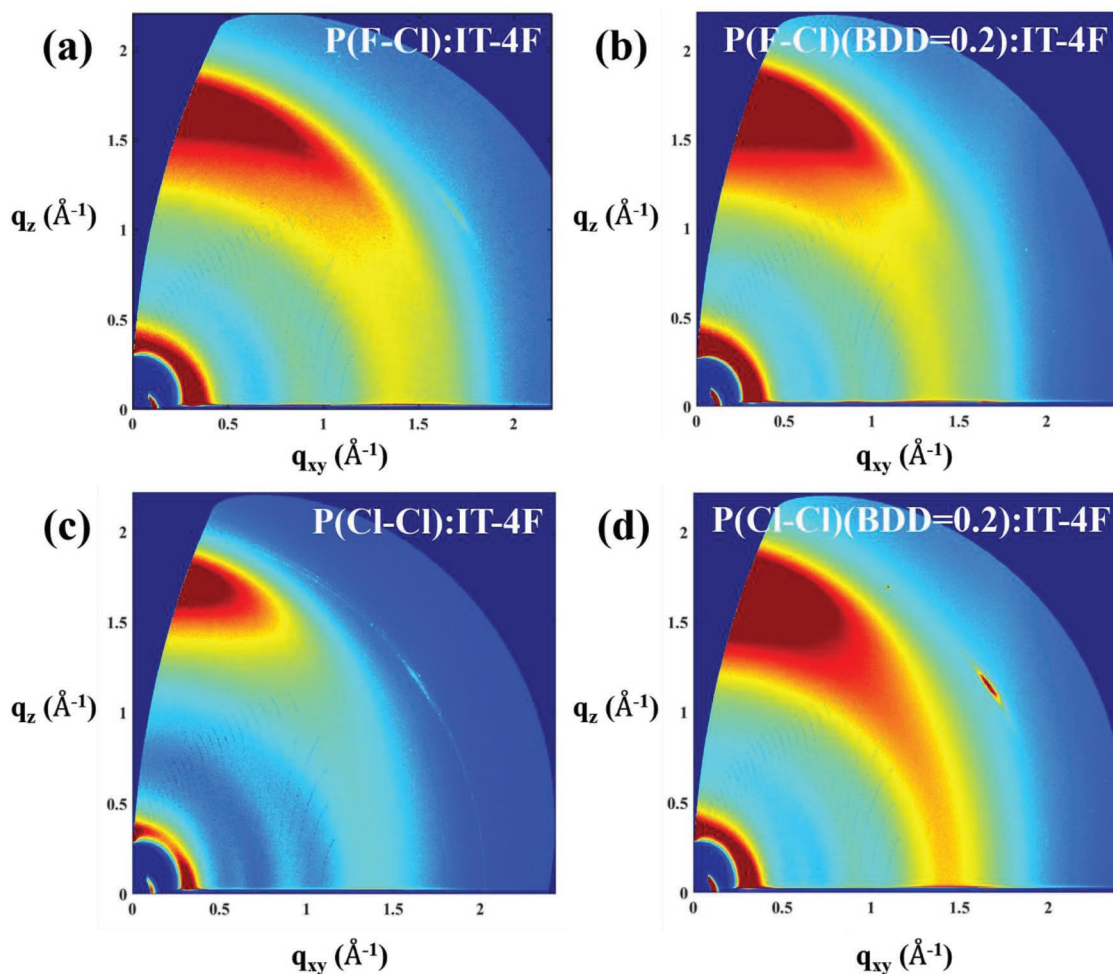

Figure 3. 2D GIWAXS patterns for optimized polymer blends of a) P(F–Cl):IT-4F, c) P(Cl–Cl):IT-4F, b) P(F–Cl)(BDD = 0.2), and d) P(Cl–Cl)(BDD = 0.2):IT-4F.

ADVANCED
SCIENCE NEWS
www.advancedsciencenews.com

NANO · MICRO
small
www.small-journal.com

Table 4. GIWAXS results for pristine active materials and optimized polymer blends in the out-of-plane (OOP) direction.

	$d[100]^{a)}$ [Å] at (100) [Å^{-1}]	$d[010]^{a)}$ [Å] at (010) [Å^{-1}]	$A_{xy}/A_z{}^{b)}$
P(F–Cl)	16.99 at 0.370	3.78 at 1.662	1.21
P(F–Cl)(BDD = 0.2)	18.84 at 0.333	3.86 at 1.629	0.95
P(Cl–Cl)	19.63 at 0.320	3.84 at 1.638	1.27
P(Cl–Cl)(BDD = 0.2)	19.75 at 0.318	3.78 at 1.664	1.11
IT-4F	16.80 at 0.374	4.11 at 1.530	1.05
P(F–Cl):IT-4F	17.90 at 0.351	3.67 at 1.711	1.46
P(F–Cl)(BDD = 0.2):IT-4F	19.76 at 0.318	3.61 at 1.740	1.00
P(Cl–Cl):IT-4F	19.50 at 0.322	3.60 at 1.744	1.13
P(Cl–Cl)(BDD = 0.2):IT-4F	19.39 at 0.324	3.59 at 1.750	1.31

$^{a)}q_{xy}$ (or q_z) = $2\pi/d[010]$ (or $d[100]$); $^{b)}$The ratio between face-on and edge-on orientations determined by the pole figure analysis, where A_{xy} and A_z correspond to the face-on and edge-on fractions, respectively.

among the optimized donor polymer blends. Therefore, the highest PCEs could be obtained with relatively high J_{sc} values. The GIWAXS analysis results and calculated values are summarized in **Table 4** and Table S3 (Supporting Information).

2.5. Morphological Characterization

The surface and microscale morphologies of the optimized polymer blends were measured using atomic force microscopy (AFM).[16,17,37] The blend films were prepared under the same conditions as those for device fabrication. As shown in **Figure** 4a–c, AFM 2D and 3D topographies of all blend films for the P(F–Cl):IT-4F (root-mean square (RMS), R_q = 0.97 nm and maximized roughness in the z-axis direction, $R_z{}^{max}$ = 12.12 nm), P(F–Cl)(BDD = 0.2):IT-4F (R_q = 0.83 nm and $R_z{}^{max}$ = 6.71 nm), and P(Cl–Cl)(BDD = 0.2):IT-4F (R_q = 1.03 nm and $R_z{}^{max}$ = 14.47 nm) were relatively smooth and uniform, except for P(Cl–Cl):IT-4F (R_q = 1.41 nm and $R_z{}^{max}$ = 20.53 nm). This finding indicated that fine phase separation and exciton transport is possible. In particular, P(F–Cl)(BDD = 0.2):IT-4F and P(Cl–Cl)(BDD = 0.2):IT-4F exhibited relatively smaller RMS and $R_z{}^{max}$ values than polymers without BDD units, thus enabling defect-free contact with the MoO_3 layer and resulting in higher FF and J_{sc} values.[21,42] On the other hand, P(Cl–Cl):IT-4F partially showed large aggregated surfaces and islands with largely separated microscale domains due to the low solubility of the polymer, resulting in relatively low FF values. Such results were consistent with the photovoltaic parameters.[42]

2.6. Charge Carrier Mobility

We measured the space-charge-limited current (SCLC) of hole-only and electron-only devices to verify the charge carrier mobility in the optimized polymer blends (Figure S18 and Table S4, Supporting Information).[17,37] The resulting electron and hole mobilities (μ_e and μ_h) were calculated using the modified Mott–Gurney equation to be, in increasing order, 4.87×10^{-4} and 1.05×10^{-4} cm^2 V^{-1} s^{-1} for P(F–Cl):IT-4F, 5.60×10^{-4} and 4.91×10^{-4} cm^2 V^{-1} s^{-1} for P(F–Cl)(BDD = 0.2):IT-4F,

1.19×10^{-4} and 2.85×10^{-4} cm^2 V^{-1} s^{-1} for P(Cl–Cl):IT-4F, and 6.11×10^{-4} and 6.76×10^{-4} cm^2 V^{-1} s^{-1} for P(Cl–Cl)(BDD = 0.2):IT-4F, respectively. Similarly, the electron/hole mobility ratios (μ_e/μ_h) are more balanced (i.e., closer to 1) with BDD. Specifically, these ratios are 4.64 and 1.14 for P(F–Cl):IT-4F and P(F–Cl)(BDD = 0.2), respectively, and 4.17 and 0.90 for P(Cl–Cl):IT-4F and P(Cl–Cl)(BDD = 0.2):IT-4F, respectively. Accordingly, introducing a small amount of BDD units to polymer backbones increased the charge carrier mobility and balance, thus contributing to their high performance in PSCs.[17,21]

2.7. Photoluminescence Analysis

Charge transfer between the donor polymers and NFAs in all the polymer blend films must be further investigated to clarify its contribution to device performance.[16,17] Photoluminescence (PL) measurement is a convenient tool for probing charge transfer or energy transfer between materials; therefore, it was performed for pristine materials and optimized polymer blends in the present study as well, respectively (Figure S19, Supporting Information). The donor polymers and NFAs exhibit PL emissions in the ranges of 570–800 and 700–880 nm, respectively; in contrast, in the polymer blends, an effective PL quenching behavior was clearly observed in the range of 700–850 nm. Most combinations of donor polymers and NFAs, except for optimized polymer blends of P(Cl–Cl):IT-4F with unbalanced HOMO energy offset, showed sufficient PL quenching rates (PLQ) at 530 and 630 nm (donor to blend (D→B) and acceptor to blend (A→B)), respectively. Specifically, the PL spectra of P(F–Cl)(BDD = 0.2):IT-4F and P(Cl–Cl)(BDD = 0.2):IT-4F revealed a highly efficient photoinduced charge transfer occurrence, with relatively high quenching rates of 95.0% and 91.6% and 77.6% and 70.7% (PLQ$_{D→B}$ and PLQ$_{A→B}$ excited at 530 nm), and 93.6% and 92.1% and 86.5% and 84.5% (PLQ$_{D→B}$ and PLQ$_{A→B}$ excited at 630 nm), respectively, as shown in **Figure 5**. These results are in good agreement with the morphology and charge carrier mobility data, which support the results of the photovoltaic parameters for optimized polymer blends. Detailed values are summarized in Table S5 (Supporting Information).
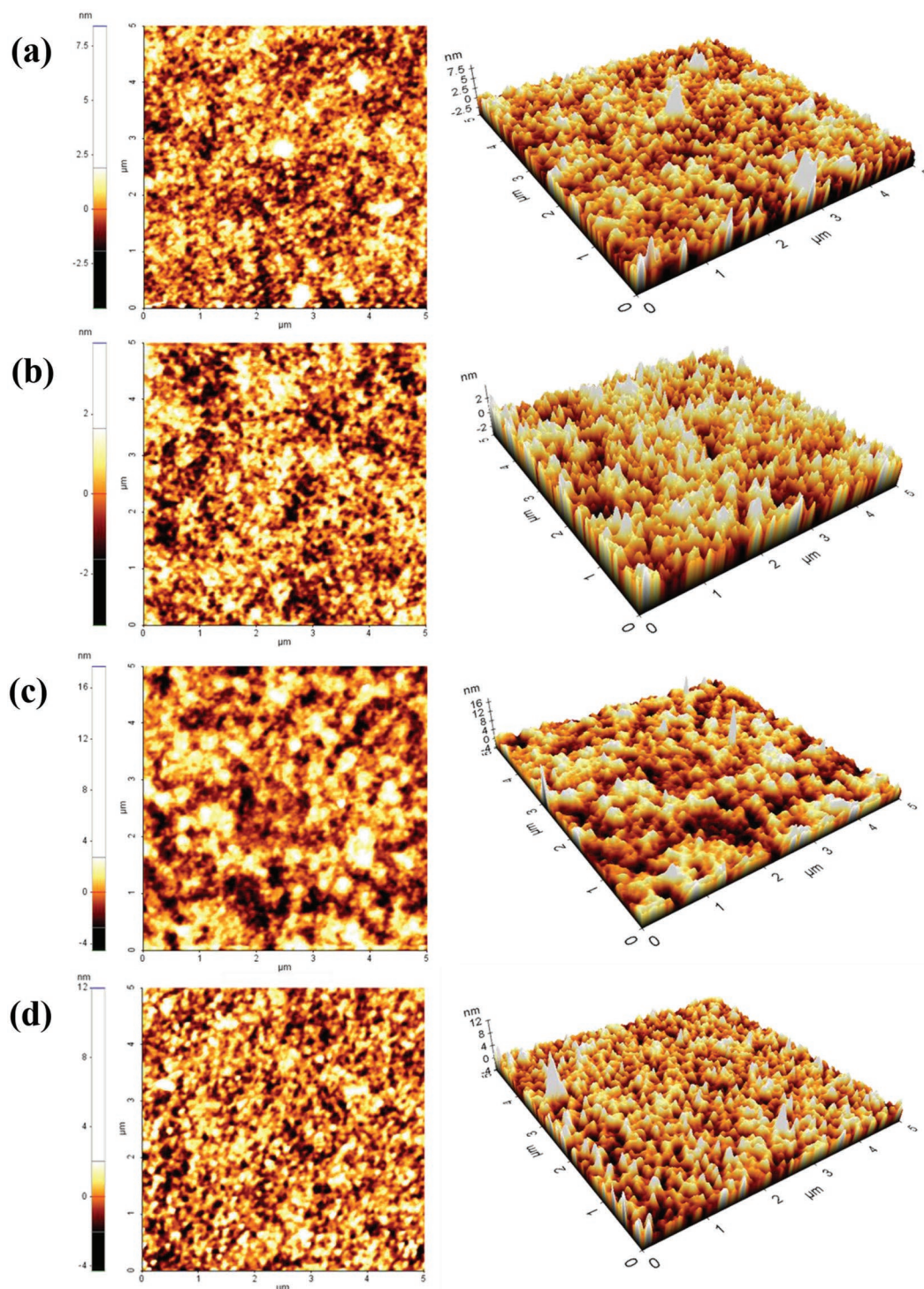
ADVANCED
SCIENCE NEWS
www.advancedsciencenews.com

NANO · MICRO
small
www.small-journal.com

Figure 4. AFM 2D and 3D topography images of the optimized polymer blends: a) P(F–Cl):IT-4F, b) P(F–Cl)(BDD = 0.2):IT-4F, c) P(Cl–Cl):IT-4F, and d) P(Cl–Cl)(BDD = 0.2):IT-4F.

2.8. Photovoltaic Performance Processed Using Eco-Friendly Solvents

We fabricated inverted PSCs with P(F–Cl)(BDD = 0.2):IT-4F and P(Cl–Cl)(BDD = 0.2), which have relatively high molecular weight and solubility, using eco-friendly solvents (XY:PN = 99.5:0.5, v/v %).

The J–V and EQE results are shown in Figure S20a,b (Supporting Information). As shown by the AFM results, both devices showed excellent photovoltaic performance despite the formation of larger domains sizes than those of PSCs fabricated using chlorinated solvents owing to the increased aggregation effect between the components (Figure S21, Supporting Information).[16,21,42,43]
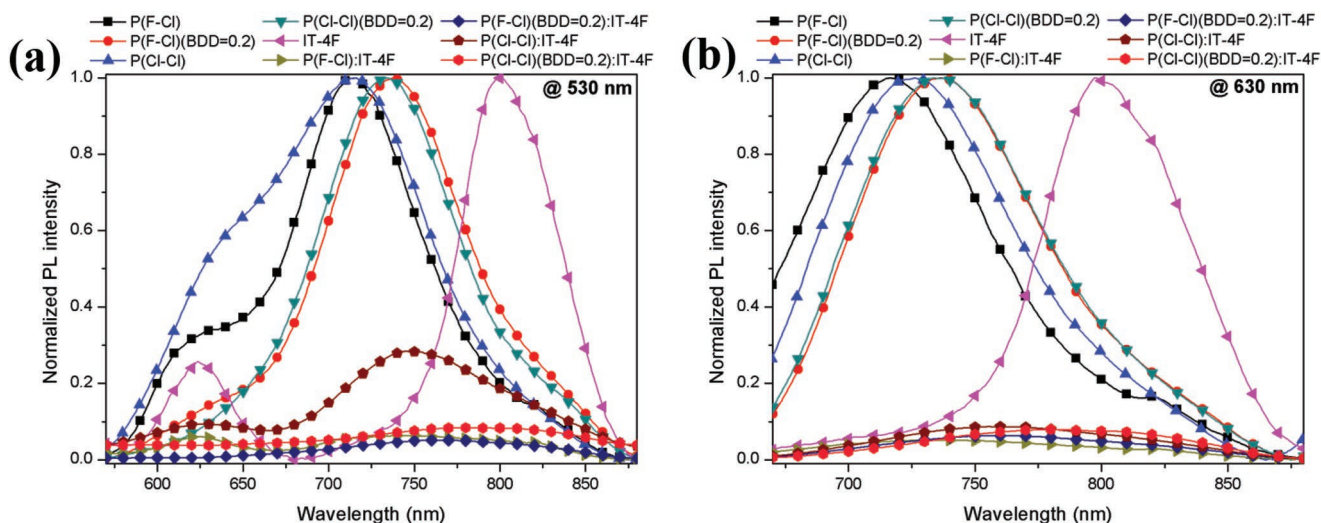
Figure 5. Normalized PL spectra of pristine materials and optimized polymer blends: the samples were excited at a) 530 nm and b) 630 nm, respectively.

Consequently, P(F–Cl)(BDD = 0.2):IT-4F showed a slightly decreased efficiency of 12.2% due to the V_{oc} and J_{sc} values, which were lower than those with chlorinated solvents. In contrast, P(Cl–Cl)(BDD = 0.2):IT-4F showed an increased efficiency of 13.5% because the FF increased more than J_{sc} decreased. These changes were because P(Cl–Cl)(BDD = 0.2):IT-4F dissolved relatively better in nonhalogenated solvents than P(F–Cl)(BDD = 0.2):IT-4F, thereby forming bi-continuous networks with balanced molecular weight and solubility. In other words, P(Cl–Cl)(BDD = 0.2):IT-4F (R_q = 1.11 nm and R_z^{max} = 10.32 nm) may have less energy loss due to its superior film morphology parameters to those of P(F–Cl)(BDD = 0.2):IT-4F (R_q = 2.61 nm and R_z^{max} = 27.54 nm).[42,43] Moreover, when both devices were certified by the Nano Convergence Practical Application Center (NCPAC) in Korea, after the devices were encapsulated, the highest PCEs of 12.70% and 13.97% were achieved, respectively, confirming the development of high-performance, eco-friendly NFPSCs (Figures S22 and S23, Supporting Information). The photovoltaic properties of the donor polymers are summarized in **Table 5**.

2.9. Photostability

In addition, we investigated the photostability of both devices with encapsulation processed by eco-friendly solvents under AM 1.5G continuous white light-emitting diode (LED) illumination. We adopted the LED as the light source instead of the xenon lamp used in the solar simulator due to light stability issues with reliability.[17] The performance of devices between the xenon the LED lamps showed a difference of ≈1% PCEs due to the each different inherent light regions. The PCEs of both cells slightly decreased below about 2.3% to 5.1% compared with each initial PCE for 30 h, which means that the both polymers-based devices have a high photostability without burn-in loss.[21] The detailed results of the measurements are shown in Figure S24 (Supporting Information).

3. Conclusion

In summary, we successfully designed and synthesized four F–2DBDT/Cl–2DBDT-chlorinated thiophene-based wide-bandgap donor polymers, P(F–Cl), P(F–Cl)(BDD = 0.2), P(Cl–Cl), and P(Cl–Cl)(BDD = 0.2), by modifying and optimizing the structure of previously reported P(Cl) to develop high-efficiency NFPSCs. To realize halogen effects for the P(F–Cl) and P(Cl–Cl), we determined that a sufficient molecular weight was required to drive their potential for structure–property. Thus, we introduced 20 mol% of a small amount of BDD into the polymer backbones as acceptor units instead of 100 mol% Cl–Th. As a result, P(F–Cl)(BDD = 0.2) and P(Cl–Cl)(BDD = 0.2) performed better than P(F–Cl) and P(Cl–Cl), not only in terms of physical, optical, and electrochemical properties but also in terms of crystallinity and orientation. In particular, the IT-4F-based PSCs for

Table 5. Optimized photovoltaic performance of the polymer blends for eco-friendly inverted PSCs.

Active Layer	Thickness [nm]	Temperature[a] [°C]	V_{oc} [V]	J_{sc} [mA cm^{-2}]	FF [%]	PCE$_{max}$/PCE$_{ave}$[b] [%]
P(F–Cl)(BDD = 0.2):IT-4F = 1:1	110	140	0.818	20.7	71.6	12.2/12.0 ± 0.18
P(F–Cl)(BDD = 0.2):IT-4F = 1:1[c]			0.813	24.06	65.0	12.70
P(Cl–Cl)(BDD = 0.2):IT-4F = 1:1	120	140	0.899	20.9	71.7	13.5/13.3 ± 0.23
P(Cl–Cl)(BDD = 0.2):IT-4F = 1:1[d]			0.891	23.40	67.0	13.97

[a]Post-annealing for 10 min; [b]Average PCE values are calculated from ten individual cells; [c]Certification result from the Nano Convergence Practical Application Center (NCPAC), Republic of Korea (No. 19S-0420); [d]Certification result from the NCPAC, Republic of Korea (No. 19S-1209).

ADVANCED
SCIENCE NEWS
www.advancedsciencenews.com

NANO · MICRO
small
www.small-journal.com

P(F–Cl)(BDD = 0.2) and P(Cl–Cl)(BDD = 0.2), which showed more balanced molecular weight and solubility, achieved higher PCEs of 12.2% (NCPAC's certified PCE: 12.70%) and 13.5% (NCPAC's certified PCE: 13.97%) when processing using eco-friendly solvents than P(F–Cl) and P(Cl–Cl). Our work provides insight into the great potential of chlorinated thiophene-based donor polymers and balancing the molecular weight and solubility of donor polymers for processing into eco-friendly NFPSCs.

4. Experimental Section

Polymerization: (Scheme S1, Supporting Information) A1 (55.3 mg, 0.20 mmol) (or A1:A2 = 0.8:0.2, mol/mol) and Pd(pph$_3$)$_4$ (8.0 mg) were added to a mixture of D1 (188.1 mg, 0.20 mmol) in a 10–20 mL vial in air. The vial was capped and vacuumed for 20 min before it was refilled with nitrogen gas, and then, anhydrous toluene (6.0 mL) and anhydrous dimethylformamide (0.6 mL) were added to the mixture. The reactor was degassed and refilled with nitrogen twice. The polymerization mixture was stirred at 100 °C for 3 h. The polymer was end-capped by the addition of 2-bromothiophenes (56.0 mg, 0.33 mmol), and the mixture was further heated at 140 °C for 1 h. After heating, 2-tributylstannyl thiophene (31.3 mg, 0.0875 mmol) was added, and the mixture was heated once more at 140 °C for 1 h. The reaction mixture was cooled to room temperature and poured into methanol (300 mL) and 37% HCl (10 mL), stirred for 1 h, and then further purified using a Soxhlet extractor with methanol, acetone, hexane, methylene chloride, ethyl acetate, chloroform, and chlorobenzene, sequentially. The chloroform fraction of the polymer was reprecipitated in methanol, filtered, and then dried under vacuum: P(F–Cl), red solid, yield: 77.0%, ^{1}H NMR (400 MHz, CDCl$_3$): Figure S1 (Supporting Information); P(F–Cl)(BDD = 0.2), violet solid, yield: 85.0%, ^{1}H NMR (400 MHz, CDCl$_3$): Figure S2 (Supporting Information); P(Cl–Cl), light red solid, yield: 72.0%, ^{1}H NMR (400 MHz, CDCl$_3$): Figure S3 (Supporting Information); P(Cl–Cl), light violet solid, yield: 89.0%, ^{1}H NMR (400 MHz, CDCl$_3$): Figure S4 (Supporting Information).

Supporting Information

Supporting Information is available from the Wiley Online Library or from the author.

Conflict of Interest

The authors declare no conflict of interest.

[1] J. Yuan, Y. Zhang, L. Zhou, G. Zhang, H.-L. Yip, T.-K. Lau, X. Lu, C. Zhu, H. Peng, P. A. Johnson, M. Leclerc, Y. Cao, J. Ulanski, Y. Li, Y. Zou, *Joule* **2019**, *3*, 1140.

[2] B. Fan, D. Zhang, M. Li, W. Zhong, Z. Zeng, L. Ying, F. Huang, Y. Cao, *Sci. China: Chem.* **2019**, *62*, 746.

[3] Q. An, X. Ma, J. Gao, F. Zhang, *Sci. Bull.* **2019**, *64*, 504.

[4] J. Yuan, T. Huang, P. Cheng, Y. Zou, H. Zhang, J. L. Yang, S. Y. Chang, Z. Zhang, W. Huang, R. Wang, D. Meng, F. Gao, Y. Yang, *Nat. Commun.* **2019**, *10*, 570.

[5] Y. Wang, X. Ke, Z. Xiao, L. Ding, R. Xia, H. Yip, *Science* **2018**, *361*, 1094.

[6] J. Hou, O. Inganas, R. H. Friend, F. Gao, *Nat. Mater.* **2018**, *17*, 119.

[7] G. Zhang, J. Zhao, P. C. Y. Chow, K. Jiang, J. Zhang, Z. Zhu, J. Zhang, F. Huang, H. Yan, *Chem. Rev.* **2018**, *118*, 3447.

[8] C. Yan, S. Barlow, Z. Wang, H. Yan, A. K. Y. Jen, S. R. Marder, X. Zhan, *Nat. Rev. Mater.* **2018**, *3*, 18003.

[9] Z. Luo, H. Bin, T. Liu, Z. Zhang, Y. Yang, C. Zhong, B. Qu, G. Li, W. Gao, D. Xie, K. Wu, Y. Sun, F. Liu, Y. Li, C. Yang, *Adv. Mater.* **2018**, *30*, 1706124.

[10] Z. Luo, T. Liu, Y. Wang, G. Zhang, R. Sun, Z. Chen, C. Zhong, J. Wu, Y. Chen, M. Zhang, Y. Zou, W. Ma, H. Yan, J. Min, Y. Li, C. Yang, *Adv. Energy Mater.* **2019**, *9*, 1900041.

[11] W. Gao, M. Zhang, T. Liu, R. Ming, Q. An, K. Wu, D. Xie, Z. Luo, C. Zhong, F. Liu, F. Zhang, H. Yan, C. Yang, *Adv. Mater.* **2018**, *30*, 1800052.

[12] J. Guo, J. Min, *Adv. Energy Mater.* **2019**, *9*, 1802521.

[13] A. Wadsworth, M. Moser, A. Marks, M. S. Little, N. Gasparini, C. J. Brabec, D. Baran, I. McCulloch, *Chem. Soc. Rev.* **2019**, *48*, 1596.

[14] R. Po, G. Bianchi, C. Carbonera, A. Pellegrino, *Macromolecules* **2015**, *48*, 453.

[15] R. Po, J. Roncali, *J. Mater. Chem. C* **2016**, *4*, 3677.

[16] J. E. Yu, S. J. Jeon, J. Y. Choi, Y. W. Han, E. J. Ko, D. K. Moon, *Small* **2019**, *15*, 1805321.

[17] S. J. Jeon, Y. W. Han, D. K. Moon, *Sol. RRL* **2019**, *3*, 1900094.

[18] Q. Fan, W. Su, Y. Wang, B. Guo, Y. Jiang, X. Guo, F. Liu, T. P. Russell, M. Zhang, Y. Li, *Sci. China: Chem.* **2018**, *61*, 531.

[19] Q. Fan, Q. Zhu, Z. Xu, W. Su, J. Chen, J. Wu, X. Guo, W. Ma, M. Zhang, Y. Li, *Nano Energy* **2018**, *48*, 413.

[20] W. Zhao, S. Li, H. Yao, S. Zhang, Y. Zhang, B. Yang, J. Hou, *J. Am. Chem. Soc.* **2017**, *139*, 7148.

[21] S. Zhang, Y. Qin, J. Zhu, J. Hou, *Adv. Mater.* **2018**, *30*, 1800868.

[22] D. Xia, Y. Wu, Q. Wang, A. Zhang, C. Li, Y. Lin, F. J. M. Colberts, J. J. Van Franeker, R. A. J. Janssen, X. Zhan, W. Hu, Z. Tang, W. Ma, W. Li, *Macromolecules* **2016**, *49*, 6445.

[23] J. Wolf, F. Cruciani, A. El Labban, P. M. Beaujuge, *Chem. Mater.* **2015**, *27*, 4184.

[24] Y. Firdaus, L. P. Maffei, F. Cruciani, M. A. Müller, S. Liu, S. Lopatin, N. Wehbe, G. O. N. Ndjawa, A. Amassian, F. Laquai, P. M. Beaujuge, *Adv. Energy Mater.* **2017**, *7*, 1700834.

[25] D. Liu, W. Zhao, S. Zhang, L. Ye, Z. Zheng, Y. Cui, Y. Chen, J. Hou, *Macromolecules* **2015**, *48*, 5172.

[26] S. Li, B. Zhao, Z. He, S. Chen, J. Yu, A. Zhong, R. Tang, H. Wu, Q. Li, J. Qin, Z. Li, *J. Mater. Chem. A* **2013**, *1*, 4508.

[27] T. Vangerven, P. Verstappen, J. Drijkoningen, W. Dierckx, S. Himmelberger, A. Salleo, D. Vanderzande, W. Maes, J. V. Manca, *Chem. Mater.* **2015**, *27*, 3726.

[28] L. Han, T. Hu, X. Bao, M. Qiu, W. Shen, M. Sun, W. Chen, R. Yang, *J. Mater. Chem. A* **2015**, *3*, 23587.

[29] H. Hu, K. Jiang, G. Yang, J. Liu, Z. Li, H. Lin, Y. Liu, J. Zhao, J. Zhang, F. Huang, Y. Qu, W. Ma, H. Yan, *J. Am. Chem. Soc.* **2015**, *137*, 14149.

[30] J. Min, Y. N. Luponosov, C. Cui, B. Kan, H. Chen, X. Wan, Y. Chen, S. A. Ponomarenko, Y. Li, C. J. Brabec, *Adv. Energy Mater.* **2017**, *7*, 1700465.

[31] C. Sun, F. Pan, H. Bin, J. Zhang, L. Xue, B. Qiu, Z. Wei, Z. G. Zhang, Y. Li, *Nat. Commun.* **2018**, *9*, 743.

[32] X. Li, F. Pan, C. Sun, M. Zhang, Z. Wang, J. Du, J. Wang, M. Xiao, L. Xue, Z. G. Zhang, C. Zhang, F. Liu, Y. Li, *Nat. Commun.* **2019**, *10*, 519.

[33] D. Qian, L. Ye, M. Zhang, Y. Liang, L. Li, Y. Huang, X. Guo, S. Zhang, Z. Tan, J. Hou, *Macromolecules* **2012**, *45*, 9611.

[34] J. Lee, J. H. Kim, B. Moon, H. G. Kim, M. Kim, J. Shin, H. Hwang, K. Cho, *Macromolecules* **2015**, *48*, 1723.

[35] Z. Li, F. Wu, H. Lv, D. Yang, Z. Chen, X. Zhao, X. Yang, *Adv. Mater.* **2015**, *27*, 6999.

[36] S. J. Jeon, S. J. Nam, Y. W. Han, T. H. Lee, D. K. Moon, *Polym. Chem.* **2017**, *8*, 2979.

[37] S. J. Jeon, Y. W. Han, D. K. Moon, *ACS Appl. Mater. Interfaces* **2019**, *11*, 9239.

[38] Z. He, C. Zhong, S. Su, M. Xu, H. Wu, Y. Cao, *Nat. Photonics* **2012**, *6*, 593.

[39] J. D. Chen, Y. Q. Li, J. Zhu, Q. Zhang, R. P. Xu, C. Li, Y. X. Zhang, J. S. Huang, X. Zhan, W. You, J. X. Tang, *Adv. Mater.* **2018**, *30*, 1706083.

[40] D. Baran, N. Gasparini, A. Wadsworth, C. H. Tan, N. Wehbe, X. Song, Z. Hamid, W. Zhang, M. Neophytou, T. Kirchartz, C. J. Brabec, J. R. Durrant, I. McCulloch, *Nat. Commun.* **2018**, *9*, 2059.

[41] B. Fan, X. Du, F. Liu, W. Zhong, L. Ying, R. Xie, X. Tang, K. An, J. Xin, N. Li, W. Ma, C. J. Brabec, F. Huang, Y. Cao, *Nat. Energy* **2018**, *3*, 1051.

[42] Y. Huang, E. J. Kramer, A. J. Heeger, G. C. Bazan, *Chem. Rev.* **2014**, *114*, 7006.

[43] G. E. Park, S. Choi, S. Y. Park, D. H. Lee, M. J. Cho, D. H. Choi, *Adv. Energy Mater.* **2017**, *7*, 1700566.